Published in final edited form as:
Neuron. 2013 February 20; 77(4): . doi:10.1016/j.neuron.2012.12.031.

Inter-axonal interaction defines tiled presynaptic innervation in *C. elegans*

Kota Mizumoto and **Kang Shen**
Howard Hughes Medical Institute, Department of Biology, Stanford University, 385 Serra Mall, California 94305, USA

Summary

Cellular interactions between neighboring axons are essential for global topographic map formation. Here we show that axonal interactions also precisely instruct the location of synapses. Motoneurons form *en passant* synapses in *Caenorhabditis elegans*. While axons from the same neuron class significantly overlap, each neuron innervates a unique and tiled segment of the muscle field by restricting its synapses to a distinct subaxonal domain—a phenomenon we term "synaptic tiling". Using DA8 and DA9 motoneurons as a model, we found that the synaptic tiling requires Plexin(PLX-1) and two transmembrane Semaphorins. In the Plexin or Semaphorin mutants, synaptic domains from both neurons expand and overlap with each other without guidance defects. In a Semaphorin-dependent manner, PLX-1 is concentrated at the synapse-free axonal segment, delineating the tiling border. Furthermore, Plexin inhibits presynapse formation by suppressing synaptic F-actin through its cytoplasmic GAP domain. Hence, contact-dependent, intra-axonal Plexin signaling specifies synaptic circuits by inhibiting synapse formation at the subcellular loci.

Introduction

Cell-cell interaction is essential for numerous events during development in multicellular organisms. Cells communicate with their neighbors by cell surface molecules including cell adhesion molecules like Cadherin and Immunoloblin (Ig) family proteins, as well as contact-dependent juxtacrine signaling molecules like Delta/Notch, Semaphorin/Plexin and Ephrin/Eph (Bray, 2006; Kullander and Klein, 2002; Takeichi, 2007; Tran et al., 2007).

In the nervous system, the construction of neural circuits critically depends on a series of developmental events including axonal growth cone migration, lamina formation and synapse formation. A large body of literature identifies several families of secreted and contact-dependent molecules, which guide growth cone migration by attractive or repulsive mechanisms (Kolodkin and Tessier-Lavigne, 2011). While long-range axon guidance is well established, the molecular mechanisms underlying local synaptic target selection have just started to be revealed (Shen and Scheiffele, 2011). Semaphorins and their receptors are two large families of conserved molecules with well-established roles guiding axon growth cones during their long-range migration (Tran et al., 2007). Recent work has also shown that Semaphorins and their receptors, Plexins, play critical roles in the establishment of local

Contact (corresponding author) Kang Shen kangshen@stanford.edu Phone: 650-724-7975 .

axonal and synaptic connectivity. In mouse retina, the transmembrane semaphorins Sema5A and Sema5B constrain neurites from multiple retinal neuron subtypes within the inner plexiform layer (IPL). Within the IPL, the repulsive interaction between another transmembrane semaphorin, Sema6A and its receptor PlexinA4 further subdivides the IPL into the ON and OFF sublaminae (Matsuoka et al., 2011b). Moreover, the secreted Sema3F inhibits synapse formation and spine morphogenesis in hippocampal granular cells and layer V cortical neurons through its receptor PlexinA3 (Tran et al., 2009). Is the ability of semaphorins to inhibit synapse formation used to create specific synaptic circuits? At least three pieces of evidence support this notion. First, Plexin A3 is also required for synapse elimination and stereotyped axon pruning of the hippocampal mossy fiber (Bagri et al., 2003; Liu et al., 2005a). Second, in the spinal cord, another secreted semaphorin, Sema3E, and its receptor Plexin-D1 prevent monosynaptic connectivity between in one specific sensory-motor circuit (Pecho-Vrieseling et al., 2009). At last, in a recent study, Ding and colleagues showed that the Sema3E and Plexin-D1 pathway specifically inhibits the thalamostriatal synapses in direct-pathway MSNs without effects on many other synapse types in the adjacent cellular environment (Ding et al., 2012). These data suggest that Semaphorins and Plexins also play important functions in establishing local synaptic connectivity and specifying target and subcellular specificity in neural circuits.

While molecular interactions between synaptic target cells including the abovementioned semaphorin signaling pathways are known to impact neural circuit assembly, axons fasciculation can also provide instructive information for precise neuronal wiring. Works in the visual and olfactory systems in *Drosophila* and mice revealed that interaction between neighboring axons is also required for precise axonal trajectories (Luo and Flanagan, 2007). Remarkably, electron microscopy reconstruction of the *C. elegans* nervous system revealed precisely patterned synaptic connections among fasciculating axons, suggesting that axon-axon interaction might also control the precise location of synapses (White et al., 1976). However, the molecular mechanisms of such regulation remain largely unknown.

To understand how inter-axonal interactions pattern synapses, we established a new system to visualize two neighboring axons of the same class and their synapses in *Caenorhabditis elegans*. The DA neurons in *C. elegans* are cholinergic motor neurons whose cell bodies reside in the ventral side and extend long axons in the dorsal nerve cord, where they form *en passant* synapses onto dorsal muscles in order to regulate backward locomotion (White et al., 1976). While DA axons largely overlap with each other in the dorsal nerve cord, each axon forms synapses selectively within a distinct axonal segment. The synaptic domains of the nine DAs cover the entire dorsal muscle field in a complete, but non-overlapping manner, thus achieving “tiled” synaptic coverage (White et al., 1976). This synaptic tiling is observed in the majority of motoneuron classes including the VA, VB, AS, DA and DB classes (White et al., 1976). To understand the molecular mechanisms underlying such synaptic tiling, we studied the DA neurons located most posteriorly, DA8 and DA9. Although the axons of DA8 and DA9 fasciculate with each other extensively in the dorsal neuropil, these two neurons form tiled synapses, with the DA8 synaptic domain always immediately anterior to that of DA9 (Figure 1A).

Using genetic manipulations, we found that DA8 and DA9 synaptic tiling is dependent on the contact between these two axons. DA8 and DA9 axons mutually inhibit each other’s synapse formation, creating tiled synaptic domains. Our genetic analysis showed that the communication between axons is mediated by an atypical Semaphorin/Plexin signaling pathway, in which Semaphorins function *in cis* to positively regulate Plexin. Plexin is enriched at the DA9 synapse-free zones in a Semaphorin-dependent manner. Plexin in turn, inhibits Ras signaling through its cytosolic GAP domain and negatively regulates presynaptic assembly by suppressing synaptic filamentous actin (F-actin).

Results

Synaptic tiling is dependent on axon-axon contact

To understand the synaptic tiling between DA8 and DA9, we differentially labeled their presynaptic specializations in two different colors using GFP and mCherry fused with the synaptic vesicle protein RAB-3. We created transgenic animals co-expressing GFP::RAB-3 under the *unc-4* promoter (active in all DA neurons) and mCherry::RAB-3 under the *mig-13* promoter (active in DA9 but not in DA8) (Klassen and Shen, 2007; Miller and Niemeyer, 1995). As a result, DA9 synapses were labeled both red and green, while DA8 synapses were labeled in green. Consistent with serial electron microscopy reconstruction (White et al., 1976), DA8 synapses (pseudocolored in green) were found anterior to DA9 synapses (pseudocolored in magenta to white due to the variable expression levels between GFP::RAB-3 and mCherry::RAB-3) with little overlap between their synaptic domains (White et al., 1976) (Figures 1B, 1C and 2A).

Since we have previously shown that diffusible gradients formed by Wnts and netrin pattern the subcellular location of synapses in the DA9 cells(Klassen and Shen, 2007; Poon et al., 2008), we first tested whether “synaptic tiling” was dependent on the general position of the cells or axon contact between DA8 and DA9. For these experiments, we examined the axon guidance mutants, *unc-34* (Enabled/VASP) and *unc-129* (TGF-β-like), which disrupt axonal contacts but retain the general cell position in the tail (Colavita and Culotti, 1998; Yu et al., 2002). In approximately 50% of *unc-34* and *unc-129* mutant animals, either the DA8 or DA9 axon failed to reach the dorsal nerve cord. It is known that, even when the axons fail to join the dorsal nerve cord due to axon guidance errors, the postsynaptic body wall muscles can still find their presynaptic axons by sending abnormally long muscle arms (Hall and Hedgecock, 1991). In animals where the DA8 and DA9 axons did not contact each other, we found that the DA8 and DA9 synaptic domains exhibit significant overlap along the A-P axis (Figures 1D and 1E). We defined DA8/DA9 overlap as a distance between the most posterior DA8 synapse and the most anterior DA9 synapse. To further understand the cause of the overlap, we measured the asynaptic domains of DA8 and DA9, as well as the length of the DA8 synaptic domain (Fig. 1A). We found that these mutants exhibit shortened DA8 asynaptic domains and lengthened DA9 synaptic domains, suggesting that the overlap of synaptic domains is caused by both the expansion of DA8 synapses posteriorly, as well as the expansion of DA9 synapses anteriorly (Figures 1B, 1D, 1E and Figure S1). In contrast, synaptic tiling was normal in mutant animals where both axons were correctly guided to the dorsal nerve cord (Figure 1B and 1F), suggesting that neither *unc-34* nor *unc-129* is essential for synaptic tiling. Instead, contact between DA8 and DA9 axons appeared critical. To definitively show that DA8 and DA9 physically contact each other, we examined the electron microscopy images and found that these two axons indeed touch each other in the posterior dorsal nerve cord (Figure S4).

The synaptic pattern is often refined by the neural activity (Sanes and Lichtman, 2001). To test whether the synaptic tiling observed in DA neurons is dependent on their neural activity, we analyzed the synaptic tiling in *unc-13* mutants. *unc-13* is required for the synaptic vesicle priming and hence the mutants of *unc-13* animals are almost completely paralyzed due to severely impaired synaptic transmission (Richmond et al., 1999). Though each synapse had more RAB-3 signal than wildtype as previously reported (Richmond et al., 1999), synaptic tiling in *unc-13* mutants was indistinguishable from that of wildtype (Figure 1B, G and Figure S1), suggesting that synaptic tiling is not dependent on the neural activities of DA neurons.

Semaphorin/Plexin signaling is responsible for the synaptic tiling

To uncover the molecular mechanisms underlying synaptic tiling, we performed a visually-based forward genetic screen for mutants with overlapping synaptic domains but normal axon guidance. Through this screen we isolated *wy592*, which showed a fully penetrant phenotype where DA8 and DA9 synapses intermingled with each other (Figure 2B and 2E). This phenotype was caused by expansion of the DA8 synaptic domain posteriorly along with expansion of the DA9 synaptic domain anteriorly, suggesting that the mutual inhibition between the DA8 and DA9 synaptic domains is significantly compromised despite appropriate axon guidance (Figure S1). We mapped this recessive mutation to a small deletion in the *plx-1* gene, which encodes the transmembrane receptor gene Plexin. The deletion introduces a premature stop codon in the PLX-1 cytoplasmic domain (Figure 2F and 3C). Similar to observations in *Drosophila* and vertebrates (Tran et al., 2007), PLX-1 functions as a receptor for members of the Semaphorin family of ligands in *C. elegans* (Fujii et al., 2002). A null allele of *plx-1*, *nc36*, was phenotypically indistinguishable from *wy592*, suggesting that *wy592* is also a null allele (Figure 2E and Figure S1). The *C. elegans* genome encodes two Plexin genes (*plx-1* and *plx-2*). *plx-2* neither displayed a synaptic tiling defect, nor enhanced the *plx-1* phenotype, suggesting that PLX-2 is not involved in DA8/9 synaptic tiling (Figure 2E and Figure S1).

The expanded RAB-3 localization could represent an expansion of the synaptic domain, or simply a mislocalization of RAB-3-containing vesicles. To address whether active zone proteins are also affected, we examined the localization of UNC-10/RIM and SYD-2/liprinα in DA9 of *plx-1* mutants. We found that both active zone markers were similarly displaced to the anterior segment of DA9 axon in the *plx-1* mutant, suggesting that the ectopic RAB-3 puncta are likely *bona fide* presynaptic specializations (Figure S2). To address whether the presynaptic position defect in the *plx-1* mutant is due to postsynaptic phenotypes, we examined the dorsal body wall muscles and did not detect obvious defect in the number and location of muscle arms and the subcellular localization of the post-synaptic acetylcholine receptor (ACR-16) in the *plx-1* mutants, possibly due to the existence of many unaffected nearby neuromuscular junctions nearby (Figure S3). Furthermore, mutants with severe defects in muscle arms development including *unc-60B*, *unc-52*, *clr-1* and *unc-73* (Alexander et al., 2009; Dixon et al., 2006; Dixon and Roy, 2005), did not show synaptic tiling defect, suggesting that synaptic tiling is not likely due to defects in the morphological patterning of the post-synaptic structures (Figure S3).

It has been reported that two transmembrane Semaphorins (SMP-1 and SMP-2) function with PLX-1 in vulva and male tail morphogenesis (Dalpe et al., 2004; Liu et al., 2005b; Nukazuka et al., 2008). Consistent with these observations, *smp-1* mutants also showed a similar, but somewhat weaker, synaptic tiling phenotype compared with *plx-1* mutants (Figure 2E). *smp-2* single mutants exhibited no synaptic tiling defect, but *smp-2;smp-1* double null mutants showed a phenotype indistinguishable from *plx-1* mutants (Figures 2C and 2E), suggesting that *smp-1* plays more important roles in synaptic tiling than *smp-2*. Furthermore, the phenotype of *smp-2;smp-1*;*plx-1* triple mutants is equivalent to that of *plx-1* single mutants, arguing that SMP-1 and SMP-2 are likely to act in the same pathway with PLX-1, with SMP-1 being the main contributor to DA motoneuron synapse tiling (Figure 2E and Figure S1). Semaphorin/Plexin signaling regulates axon guidance in many organisms, therefore we asked whether the synaptic tiling phenotypes found in the *plx-1* and *smp-1;smp-2* mutants were caused by subtle axon guidance defects. We labeled the axons of DA8 and DA9 with different colored fluorescence proteins, which allowed us to closely examine the fasciculation between the DA axons. We found no gross axon guidance defects in the *plx-1* or *smp-1;smp-2* mutants (Figure S4). Close examination of DA8 and DA9 axons revealed a stereotyped positional relationship between the two axons: in posterior dorsal

cord where DA9 form synapses, the DA9 axon was located more ventrally than the DA8 axon, while the DA8 axon occupies a more ventral position in the DA8 synaptic region anterior to the DA9 synapses (Figure S4). This precise position of DA8 and DA9 axons in the dorsal nerve cord was maintained in the *plx-1* and *smp-1;smp-2* mutants, suggesting that the synaptic tiling phenotype is not caused by the loss of axon contact between DA8 and DA9 (Figure S4). It is worth noting that the defective synaptic tiling is the first demonstration that Plexin/Semaphorin signaling is required for the development of the *C. elegans* nervous system.

Semaphorins and Plexin function *in cis* in the DA9 neuron

We next asked in which cells *plx-1* and *semaphorins* function by performing rescue experiments using several tissue-specific promoters (Figure 3, Figure S5 and S6). We used a truncated *unc-129* promoter (P*unc-129MN*) (Klassen and Shen, 2007) for expression in the DB class dorsal motoneurons; the *hlh-1* promoter (Krause et al., 1990) for expression in the body wall muscles; and a truncated *unc-4* promoter (*unc-4c*) (Wei et al., 2012) for expression in the DA motor neurons including both DA8 and DA9. While expression of PLX-1-encoding cDNA in DB class neurons or post-synaptic body wall muscles did not rescue the synaptic tiling phenotype in *plx-1* mutants, this phenotype was almost completely rescued by expressing PLX-1 in both DA8 and DA9 with a DA neuron-specific promoter (P*unc-4c*) (Figure 3A). Utilizing the mosaicism of the extrachromosomal array, we conducted genetic mosaic experiments with the P*unc-4c::plx-1* transgene to clarify in which among DA neurons PLX-1 functions. We found that mosaic animals that lost the rescuing array in DA9 did not rescue the *plx-1* mutant phenotype, suggesting that PLX-1 is required in DA9 (Figure 3A and Figure S6). Consistent with these observations, PLX-1 expressions in DA9 but not DA8 (P*mig-13*) was also sufficient to rescue the *plx-1* phenotype. Surprisingly, expression of *plx-1* in DA9 alone not only rescued the anterior expansion of the DA9 synaptic domain, but also rescued the posterior expansion of the DA8 synapses (Figures S5 and S6). We also observed partial but significant rescue with another DA9 specific promoter (P*itr-1*), which is active only in later larval stage (L3 to L4) (Figure 3A). Together, these results indicate that expression of *plx-1* in DA9 is necessary and sufficient for its function in synaptic tiling between DA8 and DA9. To further address whether PLX-1 functions as a receptor in DA9, we created deletion variants of PLX-1 and tested their rescuing activity. Deletion constructs lacking the entire extracellular region (ΔEcto), sema domain (ΔSema) or stalk domain (ΔStalk) of PLX-1 failed to rescue the *plx-* 1 mutant phenotype, consistent with the notion that PLX-1 functions as a signal-receiving receptor (Figures 3A, 3C and Figure S5).

The vast majority of the Semaphorin literature indicates that Semaphorins and their receptors function *in trans* on different cells to regulate cellular morphogenesis (Tran et al., 2007). Hence, we postulated that SMP-1 functions in DA8 to tile synapses. Surprisingly, however, the synaptic tiling phenotype in *smp-1; smp-2* double mutants could also be rescued by expression of *smp-1* in DA9, and mosaic experiments using P*unc-4c::smp-1* showed that SMP-1 was required in DA9 (Figure 3B, Figure S5 and S6). These results suggest that SMP-1, like its receptor PLX-1, functions in DA9. The rescuing effects were evident for both the DA9 synapses as well as the DA8 synapses (Figure S5), indicating that the Semaphrin/Plexin pathway is required in DA9 synapses not only to restrict the DA9 synapses, but also to pattern the DA8 synapses through an unknown mechanism. Some vertebrate Semaphorins are known to be cleaved at the extracellular region and function as secreted ligands (Tran et al., 2007). Although SMP-1 does not seem to have a conserved cleavage site in its extracellular domain, it is possible that SMP-1 in DA9 is secreted and activates PLX-1 in the same cell in an autocrine manner. Expression of a putative secreted form of SMP-1 that lacks the transmembrane and cytoplasmic domains (SMP-1(Ecto)) from

either muscle or from DA9 did not rescue the *smp-1;smp-2* mutant phenotype, suggesting that SMP-1 functions in DA9 in a membrane bound form (Figure 3B, 3C, Figure S5 and S6).

Furthermore, expression of both PLX-1 and SMP-1, but not either one alone, in DA9 (under the *mig-13* or *itr-1* promoter) was sufficient to rescue the *smp-1;smp-2;plx-1* triple mutants (Figure 3D, Figure S5 and S7). Mosaic experiment using *unc-4c* promoter showed that co-expression of PLX-1 and SMP-1 in DA9 but not in DA8 is sufficient to rescue the *smp-1;smp-2;plx-1* triple mutants, and loss of the rescuing transgene in DA9 failed to rescue the triple mutants (Figure 3D, Figure S5 and S7). This result further confirms that PLX-1 and SMP-1 act together in DA9 and are not required in other cells. Although we do not exclude the possibility that SMP-1 or/and PLX-1 also function in DA8 with unknown redundant factor(s), these results suggest that both PLX-1 and SMPs function *in cis* in DA9 to define the synaptic boundary between DA8 and DA9.

Plexin is required throughout development

The embryonically-born DA neurons complete axon guidance before the animal hatches (Sulston et al., 1983). During larval development, the length of DA axons increases dramatically as the animal lengthens. To understand when the synaptic tiling process takes place and when PLX-1 and Semaphorins are required, we examined the tiling phenotype in early L1 larvae. In wild type L1 animals, although the synaptic domains of DA8 and DA9 are much shorter than in adult, they appear to be tiled just as in the adult animals (Figure 4A). Furthermore, the *plx-1* mutant L1 larvae showed a tiling phenotype (Figure 4B). Consistent with this notion, embryonic expression of PLX-1 from a heat shock promoter (P*hsp*) significantly rescued the *plx-1* mutant phenotype, suggesting that *plx-1* is likely to be required during the formation of tiled synaptic domains (Figures 4C and 4D). Interestingly, expression of PLX-1 at later larval stages also led to partial rescue of the tiling phenotype (Figures 4C and 4D).. These results suggest that PLX-1 is mainly required to establish the synaptic tiling in early stage, but also to maintain synaptic tiling during larval growth. Other experiments in adult animals showed that there is a high turnover rate for synaptic material in DA9 synapses. In addition, another cue, LIN-44/Wnt is also required to both establish and maintain synapse position (data not shown). Therefore, it is not surprising that PLX-1 might also function to maintain synapse position.

PLX-1 is localized at the anterior edge of DA9 synaptic domain

To understand the cellular mechanisms underlying Semaphorins/PLX-1 regulation of synaptic tiling, we examined the subcellular localization patterns of these molecules in DA9. A functional SMP-1::GFP showed diffused localization throughout DA9 axon, suggestive of a permissive role of SMP-1 in DA9 (Figure 5L and 5M and data not shown). On the other hand, a functional PLX-1::GFP (data not shown) is localized to the dendrite, as well as the proximal and distal axon, but is largely absent from the synaptic domain (Figure 5A). As PLX-1 is required to restrict the presynaptic domain of DA9 at the tiling border, we examined its precise localization in relation to the presynaptic terminals. Interestingly, PLX-1::GFP and a synaptic vesicle marker exhibit a mutually exclusive localization pattern at the tiling border (Figures 5B and 5I). Together with the *plx-1* tiling phenotype, this localization pattern suggests PLX-1 inhibits the formation of presynaptic terminals in the distal DA9 axon to establish the tiling border. Consistent with this hypothesis, the sharp PLX-1::GFP border delineating the tiling border was completely dependent on axon-axon interaction: PLX-1::GFP was uniformly localized along the entire axon when assessed in DA9 neurons that exhibit aberrant axon guidance phenotypes (*unc-129* mutants) (Figures 5C and 5D). This also suggests that a signal from DA8 patterns the subcellular localization of plx-1. DA8 is not wholly responsible for patterning PLX-1 localization, however, because the PLX-1::GFP localization pattern was also completely lost in *smp-1;smp-2* mutants

(Figures 5E and 5F). Uniformly localized PLX-1::GFP in the synaptic region of *unc-129* and *smp-1;smp-2* mutants suggest that the diffused PLX-1 is not able to inhibit synapse formation, and both Semaphorins in DA9 and signal from DA8 are required to concentrate PLX-1 at the DA9 tiling border (Figure 8). In addition, the non-rescuing *plx-1* mutant protein that lacks the SEMA domain required for Semaphorin ligand binding also showed diffuse localization (Figures 5G), suggesting that Semaphorins are required to localize PLX-1 and that this specific localization pattern of PLX-1 is likely important for its function in synaptic tiling. PLX-1 that lacks its stalk region (ΔStalk) also showed no particular subcellular localization, suggesting that entire extracellular domain of PLX-1 is required for its localization (Figure 5H).

If Semaphorin and Plexins function as patterning molecules to direct the subcellular localization of synapses in DA9, we would expect that the localization of PLX-1 is independent of synaptic proteins and synaptic vesicles. Indeed, PLX-1 localization at the tiling border was observed in most *unc-104/kinesin* mutants, in which synaptic vesicles and active zones are completely absent from the DA axons (Hall and Hedgecock, 1991) (Ou et al., 2010), suggesting that PLX-1 acts upstream of presynaptic assembly to pattern synapses (Figures 5J and 5K).

PLX-1 functions as a RasGAP

It has been shown that both Plexins and transmembrane Semaphorins can transmit signals through their cytoplasmic domains (Godenschwege et al., 2002; Toyofuku et al., 2004). We next focused on the intracellular signaling of Semaphorin/Plexin in the synaptic tiling. While PLX-1 mutant protein that lacks its cytoplasmic domain (PLX-1(ΔCyto)) failed to rescue the *plx-1* mutant, SMP-1(ΔCyto) lacking its cytoplasmic domain rescued the *smp-1;smp-2* mutants as well as full-length SMP-1 (Figures 3A - 3C and Figure S5). These results indicate that PLX-1, but not SMP-1, is responsible for transmitting the intracellular signal for synaptic tiling. Like other Plexins, PLX-1 has a highly conserved RasGAP domain in its cytoplasmic region (Fujii et al., 2002; Tran et al., 2007), though its role *in vivo* remains unclear. Point mutations in the critical Arginine residues of the vertebrate PlexinA RasGAP domain completely abolish its GAP activity *in vitro* (He et al., 2009; Rohm et al., 2000). When we introduced the same mutations in the corresponding Arginine residues in PLX-1 (PLX-1(RA)), the construct was no longer able to rescue the *plx-1* mutant (Figures 3A and Figure S5). This result strongly suggests that PLX-1 inhibits presynatpic formation via its RasGAP activity. Consistent with this idea, both PLX-1(ΔCyto)::GFP and PLX-1(RA)::GFP were localized at the tiling border in *plx-1* mutants similar to wild-type PLX-1, but they failed to restrict DA9 synapse distribution, leading to ectopic synapses that overlapped with, or were anterior to PLX-1(ΔCyto)::GFP or PLX-1(RA)::GFP (Figures 6A-6E). These results suggest that the putative RasGAP activity is required for signaling but not for subcellular localization of PLX-1.

We then asked if Ras acts downstream of PLX-1 to mediate synaptic tiling. We reasoned that if loss of the RasGAP activity in PLX-1 causes a tiling phenotype, one might expect that overactive Ras would cause a similar phenotype. Indeed, we found that a gain-of-function mutant of Ras (*let-60gf*) showed a significant synaptic tiling defect (Figures 6F and 6G). To test the cellular requirement of the Ras-induced synaptic tiling phenotype, we independently expressed two dominant negative LET-60 Ras proteins (G10R and S89F) (Han and Sternberg, 1991) in DA9 using the *mig-13* promoter. We found that DA9 expression of these two Ras constructs suppressed the *let-60(gf)* mutant phenotype, suggesting that Ras also functions cell autonomously in DA9 to restrict its synaptic domain. To test if PLX-1 and let-60/Ras function in the same genetic pathway, we created *plx-1; let-60(gf)* double mutants, and found that *let-60(gf)* did not enhance the *plx-1* mutant phenotype, suggesting

that *let-60* acts in the same signaling pathway as *plx-1* in DA9 (Figure 6G). Recently it was shown that Plexin cytoplasmic domain could be a RapGAP(Wang et al., 2012). Although LET-60 is a Ras homologue, it also shows high homology to Rap family GTPases. Therefore, the incomplete synaptic tiling phenotype in the *let-60(gf)* mutants might be due to the redundant function between LET-60 and RAP homologs.

PLX-1/Ras signaling locally inhibits synaptic actin in DA9

As Ras and Plexin are well-known actin regulators (Tran et al., 2007) and we recently reported that presynaptic actin is critical for the initiation of synaptogenesis in the HSN neurons of *C. elegans* (Chia et al., 2012), it is conceivable that PLX-1 localizes immediately adjacent to the DA9 synaptic domain to restrict synapse formation via regulation of synaptic actin. We then next examined the subcellular pattern of F-actin localization in DA9 motoneurons. The Calponin-homology domain of Utrophin (Utrophin-CH), which labels presynaptic actin in HSN neurons (Chia et al., 2012), is enriched in the DA9 synaptic domain and proximal axon, but is absent from the anterior asynaptic axonal region, delineating the anterior synaptic border (Figures 7A and 7B). Though the intensity of Utrophin-CH detection is significantly reduced, its distinct subcellular localization pattern was maintained in *unc-104/kinesin3* mutants, in which the DA9 axon is completely devoid of synaptic vesicle and active zone proteins (Ou et al., 2010) (Figure 7J). This result suggests that patterning of synaptic actin occurs upstream of accumulation of synaptic vesicles and other presynaptic structural components, as observed in HSN neuron (Chia et al., 2012). Finally, we examined the Utrophin-CH staining domain in the *plx-1*, *smp-1* ;*smp-2* and *let-60(gf)* mutants and found that it was expanded in all of the tiling mutants (Figures 7C-7I). The expanded actin domain precisely colocalized with the expanded presynaptic regions labeled with mCherry::RAB-3 (Figures 7D, 7F and 7H). As *plx-1;unc-104* double mutants had a longer actin domain compared with *unc-104* mutants (Figure 7I), the expansion of the actin domain in the *plx-1* mutant is independent of synaptic materials. Together, these data suggest that PLX-1 acts in an instructive manner to define the tiling border by inhibiting DA9 presynaptic formation. PLX-1 may exert its function by restricting presynaptic actin structures via inactivation of the Ras signaling pathway (Figure 8).

Discussion

Here we established a new system to study axon-axon interaction in synaptogenesis and report the molecular mechanisms for precise patterning of the subcellular localization of synapses in *C. elegans*. We found that transmembrane Semaphorins and their receptor Plexin/PLX-1 are required to restrict synapses to the appropriate subaxonal segment. PLX-1 is enriched at the synapse-free zone immediately adjacent to the synaptic domains. Together, these data led us to propose that PLX-1 and Semaphorins inhibit synapse formation at the distal segment of DA9 axon. Inhibitors of synapse formation likely represent important mechanisms to achieve connection specificity in the construction of neural circuit *in vivo*. It is well known that synapses tend to form much more promiscuously in dissociated neuronal cultures where few extracellular cues remain, arguing that synapse formation *per se* can be achieved robustly in vitro and that inhibitory cues must suppress synaptogenesis between inappropriate neurons *in vivo* to establish correct neuronal wiring. Examples of such inhibitors include members of the Wnt family. Our previous work showed that two Wnt molecules LIN-44 and EGL-20 inhibit synapse formation at the proximal segment of DA9 (Klassen and Shen, 2007). A similar inhibitory function of a related Wnt was also reported in the wiring between motor neurons and different muscle groups in *Drosophila* (Inaki et al., 2007). In the same NMJ system, another molecule, Netrin B, has been shown to repel certain axons (Winberg et al., 1998). It should be noted that both transmembrane cues, such as

SMP-1, and diffuse gradients, including LIN-44/Wnt, play roles in patterning synaptic connections.

The actions of Semaphorins and Plexins are clearly complex. This is evident at two levels: the functional implication of Semaphorin/plexin signal (global rejection of innervation versus local regulation of synapse formation) and the cellular (pre versus postsynaptic) requirements for Plexin signaling. The transmembrane Semaphorins in the retina, Sema5 and Sema6 restrict axon arborization and hence divide the neuropil into distinct functional zones (Matsuoka et al., 2011a; Matsuoka et al., 2011b). In spinal cord, where high degree of cellular specificity between motor neurons and sensory neurons exists, Sema3E specifies cellular connectivity by inhibiting synapse formation between the cutaneous maximus (Cm) sensory neuron and the Cm motoneuron (Pecho-Vrieseling et al., 2009). In both cases, the Semaphorin signaling inhibits cellular connectivity and encodes target specificity. Interestingly, in several other cases, the semaphorin signaling also appears to regular local synaptic connectivity in a subcellular level. For example, in the hippocampal pyramidal cells, Neuropilin2 is localized at in the primary apical dendrite where it inhibits spine formation (Tran et al., 2009). Ding and colleague showed that inactivation of Sema3E/Plexin-D1 system caused selectively enhanced thalamostriatal innervation of the direct-pathway medium spiny neurons. Since the number of dendritic spines on these neurons is not significantly increased, the Sema3E system is likely to regulate the subcellular localization of synapses onto dendritic spines, shaft or cell body (Ding et al., 2012). Our data also showed that locally enriched PLX-1 inhibits synapse formation, suggesting a conserved role of Plexin across species.

In the vast majority of cases, Semaphorins and their receptors functions *in trans* to modulate cellular morphology. However, our cell autonomy results suggest that SMP-1 functions with PLX-1 *in cis* to regulate subcellular localization of PLX-1. It has been reported that some transmembrane-ligands, including Sema6A, function in the same cells as their receptors to inhibit receptor activation by competing with the trans-expressed ligands or through unknown mechanisms (Axelrod, 2010; Haklai-Topper et al., 2010; Yaron and Sprinzak, 2012). Our results are the first demonstration, to our knowledge, that a Semaphorin activates its receptor in the same cell. There are two possible ways to achieve this *cis*-activation. The first model places Semaphorin as an activator of PLX-1 in DA9. Binding between Semaphorin and PLX-1 *in cis* may cause a conformational change in the PLX-1 extracellular domain that allows the access of another interacting partner expressed in the other neuron, DA8. The second model is that SMP-1 might function as a co-receptor for Plexin in worms. Vertebrate Plexin requires its co-receptor, Neuropilin, in order to bind a secreted form of Semaphorin (Takahashi et al., 1999; Tran et al., 2007). There is no clear homolog of Neuropilin in *C. elegans* genome, but it is possible that PLX-1 and SMP-1 in the same cell form a single receptor complex to interact with unknown molecules in DA8 to achieve synaptic tiling. Both models speculate that the PLX-1 pattern in DA9 is instructed by a factor in DA8, which is supported by the observation that the PLX-1 subcellular localization at the synaptic tiling border is completely disrupted in the absence of DA8-DA9 contact (Figure 5C and 5D). Interestingly, PLX-1 or SMP-1 must also send a signal back to the DA8 neuron to regulate its synapse pattern (Figure 8). This is evident from two sets of results. First, in *plx-1* or *smp-1* mutants, not only DA9 showed abnormally expanded synaptic domains, DA8 also forms ectopic synapses (Figure S1). Second, cell autonomous expression of PLX-1 or SMP-1 in DA9 not only rescues the synaptic phenotype in DA9 in corresponding mutants, but also rescues the phenotypes in DA8 neurons (Figure S5 and S6). Identification of the molecules that function in the DA8 neuron and interact with SMP-1/PLX-1 in DA9 should help to elucidate the precise molecular mechanisms of axon-axon interaction-dependent synaptic tiling.

The assembly of presynaptic specializations involves recruitment of macromolecular active zone complex and synaptic vesicles to the synaptic membrane, a cellular process that is distinct from the turning of a growth cone or the growth and retraction of dendritic spines. How could these three different biological processes be regulated by the same set of molecular cues? It appears that the answer might be found at a common cytoskeleton component required for axon guidance, presynapse formation and dendritic spine formation: filamentous actin (F-actin). It is well documented that F-actin dynamics are key to axon growth cone turning and dendritic spine dynamics (Hotulainen and Hoogenraad, 2010; Lowery and Van Vactor, 2009). Our recent work on another *C. elegans* neuron, HSN, showed that F-actin also plays an important role in presynaptic development *in vivo* (Chia et al., 2012). consistent with previous reports in cultured neurons (Zhang and Benson, 2001). It appears that F-actin is patterned by the synaptic specificity cues and in turn recruits active zone proteins through scaffold adaptor proteins. In HSN, presynaptic F-actin is induced by the synaptic adhesion molecule SYG-1/kirrel1, which promotes local synapse formation (Chia et al., 2012). Interestingly, in DA9, Plexin inhibits F-actin and prevents synapse formation by inactivating the small GTPase RAS. Hence, it is conceivable that synapse promoting and inhibiting cues act in concert to determine the pattern of synapses by converging on F-actin regulation, a theme that has been proposed for axon guidance. A recent study showed that inhibition of the small G protein Rac1 by the Rac GTPase-activating protein β2-Chimaerin mediated Sema3F-dependent axon pruning but was dispensable for axon repulsion and spine remodeling (Riccomagno et al., 2012). Taken together, these results suggest that differential regulation of actin dynamics by diverse actin modifying pathways might underlie the multiple functional outcomes of various Semaphorins.

In addition, we demonstrate that local axon-axon interactions are critical to establish precise presynaptic patterning. A previous study showed that subcellular compartmentalization of membrane proteins can be achieved cell autonomously in cultured Drosophila neurons (Katsuki et al., 2009). Our experiments provide evidence that synaptic domains can also be patterned using information between fasciculating axons. Although precise positional control of synaptic assembly through inter-axonal communication at the single synapse level has not yet been documented in mammals, subcellular localization of presynaptic specializations is regulated among fasciculating axons on the mossy fibers of hippocampus (Deguchi et al., 2011). Furthermore, axon-axon interaction is clearly important for the wiring of the olfactory central nervous system in both *Drosophila* and mouse (Luo and Flanagan, 2007; Sakano, 2010). Lastly, we note that the intra-axonal presynaptic “tiling” restricts synaptic innervation among neuronal groups is similar to that observed for the tiling of axonal and dendritic processes by the homotypic repulsive molecule DSCAM and DSCAM2 (Fuerst et al., 2008; Millard et al., 2007; Ting et al., 2007). Thus, synaptic tiling provides an alternative way to achieve maximal, non-overlapping synaptic innervation.

Experimental Procedures

Strains and genetics

Worms were raised on OP50 *Escherichia coli*-seeded nematode growth medium (NGM) plates at 20 °C. The following mutant strains were obtained through the Caenorhabditis Genetics Center: NW987 *unc-129(ev554)IV*, ST36 *plx-1(nc36)IV*, ST60 *gcn-1(nc40)III*, NW1702 *smp-1(ev715)I*, NW1704 *smp-2(ev709)I;jcIs1IV; him5(e1490)V*, MT2124 *let-60(n1046gf)*, CB450 *unc-13(e450)I*. The following strain is provided by G. Garriga: NG3072 *unc-34(gm104)V*. The following strain was provided by S. Mitani: TV1262 *plx-2(tm729)II*. Bristol N2 was used as the wildtype reference strain(Brenner, 1974).

Fluorescence microscopy and confocal imaging

Images of fluorescently tagged fusion proteins were captured in live *C. elegans* using a Zeiss LSM710 confocal microscope (Carl Zeiss, Germany). Worms were immobilized on 2% agarose pad using 10 mM levamisole (Sigma-Aldrich). Images were analyzed with Zen software (Carl Zeiss) or Image J (NIH, USA).

Quantification of average DA8/DA9 overlap, DA8 asynaptic domain, DA9 synaptic domain and synaptic actin domain

We defined each parameter as follows; DA8/9 overlap: a distance between the most anterior DA9 synapse and the most posterior DA8 synapse, DA8 asynaptic domain: a distance from commissure to the most posterior DA8 synapse, DA9 synaptic domain: a distance between the most anterior and posterior DA9 synapses. To normalize the body length, only middle L4 (judged by the stereotyped shape of developing vulva) animals were scored. Averages were taken from at least 20 samples. For GFP::Utrophin-CH, we measured the length from the posterior end of dorsal axon to the anterior end of GFP::Utrophin-CH domain, as there is no clear relationship between the posterior end of DA9 synaptic domain and the posterior border of GFP::Utrophin-CH.

Mosaic experiment

In order to visualize the transgene in DA9 of the *plx*-1 mutants and *smp-1;smp-2* double mutants, we used arrays containing either P*unc-4c::plx-1* or *Punc-4c::smp-1* with DA9 marker, P*mig-13::myr-mCherry*. In most transgenic animals, DA9 expressed myr-mCherry, which indicated the presence of transgenes in DA9. We quantified the animals that have lost the transgene in DA9 (identified as no myr-mCherry expression in DA9). For the mosaic experiments in the *smp-1;smp-2;plx-1* triple mutants, we used arrays containing P*unc-4c::smp-1*, P*unc-4c::plx-1* and P*unc-4::histone::mCherry*. Presence of array in DA8 and/or DA9 was judged by the nuclear Histone::mCherry signal.

Heat shock experiment

Animals were cultured at 20 degree for multiple generations to ensure there is no leaky expression from *hsp* promoter. Plates with experimental animals in embryonic or L2-L3 stages were placed at 30 degree for 3 hours and put them back to 20 degree until animals grew up to L4 stage. Animals without transgene in the same plates were also quantifies as controls.

Cloning and constructs

Expression clones were made in a derivative of pPD49.26 (A. Fire), the pSM vector (kind gift from S. McCarroll and C. I. Bargmann). Primer sets used in this study were listed in the supplemental Experimental Procedures. The following plasmids and strains were generated using standard techniques: *wyIs222* (P*unc-4::gfp::rab-3;* P*mig- 13::mCherry::rab-3*), *wyIs320* (P*itr-1::plx-1::gfp;* P*mig-13::mCherry::rab-3*) , *wyIs329* (P*mig-13::gfp::utrophin-ch;* P*mig-13::mCherry::rab-3*), *wyEx802* (P*myo-3::acr-16::gfp;* P*mig-13::mcherry::rab-3*), *wyEx3398, 3399* (P*hlh-1::plx-1*), *wyEx3726, 3800* (P*unc-129::plx-1*), *wyEx3719, 3720* (P*unc-4c::plx-1*), *wyEx4387, 4388* (P*unc-4c::plx-1;*P*mig-13::myr-mCherry*), *wyEx3721, 3722* (P*mig-13::plx-1*), *wyEx5217, 5219* (P*itr-1::plx-1*), *wyEx4284, 4285* (P*mig-13::plx-1(*Δ*sema)*), *wyEx4498, 4499* (P*mig-13::plx-1(*Δ*ecto)*), *wyEx4386, 4418* (P*mig-13::plx-1(*Δ*stalk)*), *wyEx4511, 4358* (P*mig-13::plx-1(*Δ*cyto)*), *wyEx4384, 4385* (P*mig-13::plx-1(RA)*), *wyEx4580, 4581* (P*hsp::plx-1*), *wyEx4086, 4087* (P*hlh-1::smp-1*), *wyEx4081, 4082* (P*unc-129::smp-1*), *wyEx3784, 4088* (P*mig-13::smp-1*), *wyEx3799, 3986* (P*unc-4c::smp-1*), *wyEx4222, 4223* (P*unc-4c::smp-1;* P*mig-13::myr-mCherry*), *wyEx3781, 3782* (P*mig-13::smp-1(ecto)*), *wyEx3783* (P*hlh-1::smp-1(ecto)*), *wyEx4220, 4221*

(P*mig-13::smp-1(Δcyto)*), *wyEx5017, 5018* (P*mig-13::plx-1;* P*mig-13::smp-1*), *wyEx5257, 5258* (P*unc-4c::smp-1;* P*unc-4c::plx-1;* P*unc-4::histone::mCherry*), *wyEx4902* (P*itr-1::plx-1(RA)::gfp;* P*mig-13::mCherry::rab-3*), *wyEx4010* (P*itr-1::plx-1(Δsema)::gfp;* P*mig-13::mCherry::rab-3*), *wyEx5078* (P*itr-1::plx-1(Δstalk)::gfp;* P*mig-13::mCherry::rab-3*), *wyEx4904* (P*itr-1::plx-1(Δcyto)::gfp;* P*mig-13::mCherry::rab-3*), *wyEx5266* (P*itr-1::smp-1::gfp;* P*mig-13::mCherry::rab-3*), *wyEx4626* (P*mig-13::let-60(G10R)*), *wyEx4628* (P*mig-13::let-60(S89F)*).

We used the co-injection markers P*odr-1::GFP* injected at 20 ng/μl; worms were transformed as previously described (Mello et al., 1991). *wyIs222* carries P*odr-1::dsRED* as a transgene marker. Expressions of each deletion construct were confirmed by the expression patterns of GFP-fused versions (data not shown).

***plx-1, smp-1* and *let-60* cDNA cloning—**N2 total RNA was isolated from mixed stage N2 animals using TRIzol (Invitrogen). cDNA library was prepared from N2 total RNA using Superstcipt III (Invitrogen). All genes were amplified from cDNA libraries with Phusion polymerase (Finnzymes) and gene-specific primer sets. cDNAs were subcloned into *Asc*I/*Kpn*I sites of the pSM vector with (*plx-1*) or without GFP (*plx-1, smp-1* and *let-60*). All amplified fragment were sequenced. Each promoter sequence was inserted into *Sph*I/*Asc*I sites.

***hlh-1* promoter—**Approximately 3 kb promoter region of *hlh-1* gene was amplified from N2 genomic DNA with Phusion polymerase and specific primer sets. Amplified fragments were cloned into *Sph*I/*Asc*I sites of pSM vector and partially sequenced. P*hlh-1::myr-GFP* was generated to see the expression pattern of *hlh-1* promoter and confirmed that it was expressed in all body wall muscles but not in neurons (data not shown).

Supplementary Material

Refer to Web version on PubMed Central for supplementary material.

Acknowledgments

We thank A. Kolodkin for sharing unpublished results and critical comments on the manuscript, D Hall for the EM image, the International Caenorhabditis Genetic Center, S. Mitani (National BioResource Project, JAPAN) and G. Garriga for strains. We also thank A. Howell, M. Klassen, O. Liu and G. Maro for comments on the manuscript. This work is supported by the Human Frontier Science Program fellowship (K.M.), the Japan Society for the Promotion of Science (K.M.), the Howard Hughes Medical Institute (K.S.), the Human Frontier Science Foundation (K.S.) and the W. Keck Foundation (K.S.). K.M. is also supported partly by the Leave-a-nest grant.

References

Alexander M, Chan KK, Byrne AB, Selman G, Lee T, Ono J, Wong E, Puckrin R, Dixon SJ, Roy PJ. An UNC-40 pathway directs postsynaptic membrane extension in Caenorhabditis elegans. Development. 2009; 136:911–922. [PubMed: 19211675]

Axelrod JD. Delivering the lateral inhibition punchline: it's all about the timing. Sci Signal. 2010; 3:pe38. [PubMed: 20978236]

Bagri A, Cheng HJ, Yaron A, Pleasure SJ, Tessier-Lavigne M. Stereotyped pruning of long hippocampal axon branches triggered by retraction inducers of the semaphorin family. Cell. 2003; 113:285–299. [PubMed: 12732138]

Bray SJ. Notch signalling: a simple pathway becomes complex. Nat Rev Mol Cell Biol. 2006; 7:678–689. [PubMed: 16921404]

Brenner S. The genetics of Caenorhabditis elegans. Genetics. 1974; 77:71–94. [PubMed: 4366476]

Chia PH, Patel MR, Shen K. NAB-1 instructs synapse assembly by linking adhesion molecules and F-actin to active zone proteins. Nat Neurosci. 2012; 15:234–242. [PubMed: 22231427]

Colavita A, Culotti JG. Suppressors of ectopic UNC-5 growth cone steering identify eight genes involved in axon guidance in Caenorhabditis elegans. Dev Biol. 1998; 194:72–85. [PubMed: 9473333]

Dalpe G, Zhang LW, Zheng H, Culotti JG. Conversion of cell movement responses to Semaphorin-1 and Plexin-1 from attraction to repulsion by lowered levels of specific RAC GTPases in C. elegans. Development. 2004; 131:2073–2088. [PubMed: 15073148]

Deguchi Y, Donato F, Galimberti I, Cabuy E, Caroni P. Temporally matched subpopulations of selectively interconnected principal neurons in the hippocampus. Nat Neurosci. 2011; 14:495–504. [PubMed: 21358645]

Ding JB, Oh WJ, Sabatini BL, Gu C. Semaphorin 3E-Plexin-D1 signaling controls pathway-specific synapse formation in the striatum. Nat Neurosci. 2012; 15:215–223. [PubMed: 22179111]

Dixon SJ, Alexander M, Fernandes R, Ricker N, Roy PJ. FGF negatively regulates muscle membrane extension in Caenorhabditis elegans. Development. 2006; 133:1263–1275. [PubMed: 16495308]

Dixon SJ, Roy PJ. Muscle arm development in Caenorhabditis elegans. Development. 2005; 132:3079–3092. [PubMed: 15930100]

Fuerst PG, Koizumi A, Masland RH, Burgess RW. Neurite arborization and mosaic spacing in the mouse retina require DSCAM. Nature. 2008; 451:470–474. [PubMed: 18216855]

Fujii T, Nakao F, Shibata Y, Shioi G, Kodama E, Fujisawa H, Takagi S. Caenorhabditis elegans PlexinA, PLX-1, interacts with transmembrane semaphorins and regulates epidermal morphogenesis. Development. 2002; 129:2053–2063. [PubMed: 11959816]

Godenschwege TA, Hu H, Shan-Crofts X, Goodman CS, Murphey RK. Bi-directional signaling by Semaphorin 1a during central synapse formation in Drosophila. Nat Neurosci. 2002; 5:1294–1301. [PubMed: 12436113]

Haklai-Topper L, Mlechkovich G, Savariego D, Gokhman I, Yaron A. Cis interaction between Semaphorin6A and Plexin-A4 modulates the repulsive response to Sema6A. EMBO J. 2010; 29:2635–2645. [PubMed: 20606624]

Hall DH, Hedgecock EM. Kinesin-related gene unc-104 is required for axonal transport of synaptic vesicles in C. elegans. Cell. 1991; 65:837–847. [PubMed: 1710172]

Han M, Sternberg PW. Analysis of dominant-negative mutations of the Caenorhabditis elegans let-60 ras gene. Genes Dev. 1991; 5:2188–2198. [PubMed: 1748278]

He H, Yang T, Terman JR, Zhang X. Crystal structure of the plexin A3 intracellular region reveals an autoinhibited conformation through active site sequestration. Proc Natl Acad Sci U S A. 2009; 106:15610–15615. [PubMed: 19717441]

Hotulainen P, Hoogenraad CC. Actin in dendritic spines: connecting dynamics to function. J Cell Biol. 2010; 189:619–629. [PubMed: 20457765]

Inaki M, Yoshikawa S, Thomas JB, Aburatani H, Nose A. Wnt4 is a local repulsive cue that determines synaptic target specificity. Curr Biol. 2007; 17:1574–1579. [PubMed: 17764943]

Katsuki T, Ailani D, Hiramoto M, Hiromi Y. Intra-axonal patterning: intrinsic compartmentalization of the axonal membrane in Drosophila neurons. Neuron. 2009; 64:188–199. [PubMed: 19874787]

Klassen MP, Shen K. Wnt signaling positions neuromuscular connectivity by inhibiting synapse formation in C. elegans. Cell. 2007; 130:704–716. [PubMed: 17719547]

Kolodkin AL, Tessier-Lavigne M. Mechanisms and molecules of neuronal wiring: a primer. Cold Spring Harb Perspect Biol. 2011:3.

Krause M, Fire A, Harrison SW, Priess J, Weintraub H. CeMyoD accumulation defines the body wall muscle cell fate during C. elegans embryogenesis. Cell. 1990; 63:907–919. [PubMed: 2175254]

Kullander K, Klein R. Mechanisms and functions of Eph and ephrin signalling. Nat Rev Mol Cell Biol. 2002; 3:475–486. [PubMed: 12094214]

Liu XB, Low LK, Jones EG, Cheng HJ. Stereotyped axon pruning via plexin signaling is associated with synaptic complex elimination in the hippocampus. J Neurosci. 2005a; 25:9124–9134. [PubMed: 16207871]

Liu Z, Fujii T, Nukazuka A, Kurokawa R, Suzuki M, Fujisawa H, Takagi S. C. elegans PlexinA PLX-1 mediates a cell contact-dependent stop signal in vulval precursor cells. Dev Biol. 2005b; 282:138–151. [PubMed: 15936335]

Lowery LA, Van Vactor D. The trip of the tip: understanding the growth cone machinery. Nat Rev Mol Cell Biol. 2009; 10:332–343. [PubMed: 19373241]

Luo L, Flanagan JG. Development of continuous and discrete neural maps. Neuron. 2007; 56:284–300. [PubMed: 17964246]

Matsuoka RL, Chivatakarn O, Badea TC, Samuels IS, Cahill H, Katayama K, Kumar SR, Suto F, Chedotal A, Peachey NS, et al. Class 5 transmembrane semaphorins control selective Mammalian retinal lamination and function. Neuron. 2011a; 71:460–473. [PubMed: 21835343]

Matsuoka RL, Nguyen-Ba-Charvet KT, Parray A, Badea TC, Chedotal A, Kolodkin AL. Transmembrane semaphorin signalling controls laminar stratification in the mammalian retina. Nature. 2011b; 470:259–263. [PubMed: 21270798]

Mello CC, Kramer JM, Stinchcomb D, Ambros V. Efficient gene transfer in C.elegans: extrachromosomal maintenance and integration of transforming sequences. EMBO J. 1991; 10:3959–3970. [PubMed: 1935914]

Millard SS, Flanagan JJ, Pappu KS, Wu W, Zipursky SL. Dscam2 mediates axonal tiling in the Drosophila visual system. Nature. 2007; 447:720–724. [PubMed: 17554308]

Miller DM 3rd, Niemeyer CJ. Expression of the unc-4 homeoprotein in Caenorhabditis elegans motor neurons specifies presynaptic input. Development. 1995; 121:2877–2886. [PubMed: 7555714]

Nukazuka A, Fujisawa H, Inada T, Oda Y, Takagi S. Semaphorin controls epidermal morphogenesis by stimulating mRNA translation via eIF2alpha in Caenorhabditis elegans. Genes Dev. 2008; 22:1025–1036. [PubMed: 18413715]

Ou CY, Poon VY, Maeder CI, Watanabe S, Lehrman EK, Fu AK, Park M, Fu WY, Jorgensen EM, Ip NY, et al. Two cyclin-dependent kinase pathways are essential for polarized trafficking of presynaptic components. Cell. 2010; 141:846–858. [PubMed: 20510931]

Pecho-Vrieseling E, Sigrist M, Yoshida Y, Jessell TM, Arber S. Specificity of sensory-motor connections encoded by Sema3e-Plxnd1 recognition. Nature. 2009; 459:842–846. [PubMed: 19421194]

Poon VY, Klassen MP, Shen K. UNC-6/netrin and its receptor UNC-5 locally exclude presynaptic components from dendrites. Nature. 2008; 455:669–673. [PubMed: 18776887]

Riccomagno MM, Hurtado A, Wang HB, Joshua GJ, Macopson JGJ, Griner EM, Betz A, Brose N, Kazanietz MG, Kolodkin AL. The RacGAP β2-Chimaerin selectively mediates axonal pruning in the hippocampus. Cell. 2012 in press.

Richmond JE, Davis WS, Jorgensen EM. UNC-13 is required for synaptic vesicle fusion in C. elegans. Nat Neurosci. 1999; 2:959–964. [PubMed: 10526333]

Rohm B, Rahim B, Kleiber B, Hovatta I, Puschel AW. The semaphorin 3A receptor may directly regulate the activity of small GTPases. FEBS Lett. 2000; 486:68–72. [PubMed: 11108845]

Sakano H. Neural Map Formation in the Mouse Olfactory System. Neuron. 2010; 67:530–542. [PubMed: 20797531]

Sanes JR, Lichtman JW. Induction, assembly, maturation and maintenance of a postsynaptic apparatus. Nat Rev Neurosci. 2001; 2:791–805. [PubMed: 11715056]

Shen K, Scheiffele P. Genetics and cell biology of building specific synaptic connectivity. Annu Rev Neurosci. 2011; 33:473–507. [PubMed: 20367446]

Sulston JE, Schierenberg E, White JG, Thomson JN. The embryonic cell lineage of the nematode Caenorhabditis elegans. Dev Biol. 1983; 100:64–119. [PubMed: 6684600]

Takahashi T, Fournier A, Nakamura F, Wang LH, Murakami Y, Kalb RG, Fujisawa H, Strittmatter SM. Plexin-neuropilin-1 complexes form functional semaphorin-3A receptors. Cell. 1999; 99:59–69. [PubMed: 10520994]

Takeichi M. The cadherin superfamily in neuronal connections and interactions. Nat Rev Neurosci. 2007; 8:11–20. [PubMed: 17133224]

Ting CY, Herman T, Yonekura S, Gao S, Wang J, Serpe M, O'Connor MB, Zipursky SL, Lee CH. Tiling of r7 axons in the Drosophila visual system is mediated both by transduction of an activin signal to the nucleus and by mutual repulsion. Neuron. 2007; 56:793–806. [PubMed: 18054857]

Toyofuku T, Zhang H, Kumanogoh A, Takegahara N, Yabuki M, Harada K, Hori M, Kikutani H. Guidance of myocardial patterning in cardiac development by Sema6D reverse signalling. Nat Cell Biol. 2004; 6:1204–1211. [PubMed: 15543137]

Tran TS, Kolodkin AL, Bharadwaj R. Semaphorin regulation of cellular morphology. Annu Rev Cell Dev Biol. 2007; 23:263–292. [PubMed: 17539753]

Tran TS, Rubio ME, Clem RL, Johnson D, Case L, Tessier-Lavigne M, Huganir RL, Ginty DD, Kolodkin AL. Secreted semaphorins control spine distribution and morphogenesis in the postnatal CNS. Nature. 2009; 462:1065–1069. [PubMed: 20010807]

Wang Y, He H, Srivastava N, Vikarunnessa S, Chen YB, Jiang J, Cowan CW, Zhang X. Plexins are GTPase-activating proteins for Rap and are activated by induced dimerization. Sci Signal. 2012; 5:ra6. [PubMed: 22253263]

Wei X, Potter CJ, Luo L, Shen K. Controlling gene expression with the Q repressible binary expression system in Caenorhabditis elegans. Nature methods. 2012; 9:391–395. [PubMed: 22406855]

White JG, Southgate E, Thomson JN, Brenner S. The structure of the ventral nerve cord of Caenorhabditis elegans. Philos Trans R Soc Lond B Biol Sci. 1976; 275:327–348. [PubMed: 8806]

Winberg ML, Mitchell KJ, Goodman CS. Genetic analysis of the mechanisms controlling target selection: complementary and combinatorial functions of netrins, semaphorins, and IgCAMs. Cell. 1998; 93:581–591. [PubMed: 9604933]

Yaron A, Sprinzak D. The cis side of juxtacrine signaling: a new role in the development of the nervous system. Trends Neurosci. 2012; 35:230–239. [PubMed: 22222351]

Yu TW, Hao JC, Lim W, Tessier-Lavigne M, Bargmann CI. Shared receptors in axon guidance: SAX-3/Robo signals via UNC-34/Enabled and a Netrin-independent UNC-40/DCC function. Nat Neurosci. 2002; 5:1147–1154. [PubMed: 12379860]

Zhang W, Benson DL. Stages of synapse development defined by dependence on F-actin. J Neurosci. 2001; 21:5169–5181. [PubMed: 11438592]

Highlights

- First in depth description and molecular characterization of ‘synaptic tiling’
- New system to study axon-axon interaction *in vivo*
- Role of Semaphorin/Plexin signaling in synaptic patterning independent of axon guidance
- Extracellular cues inhibit synapse formation possibly through regulating synaptic F-actin

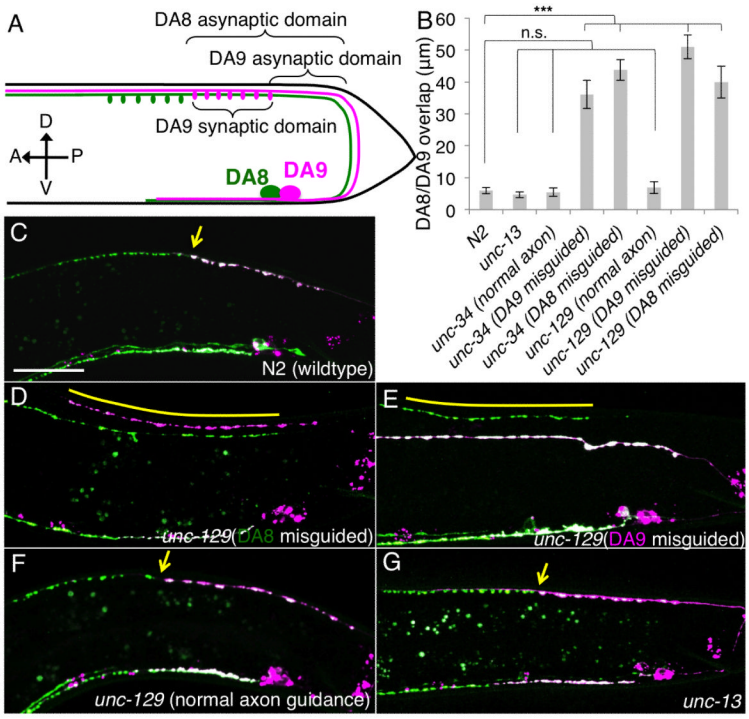

Figure 1. DA8/DA9 synaptic tiling depends on axon-axon interaction

(A) Schematic representative of the DA8 (green) and DA9 (magenta) neuron. Cell bodies are shown as big circles, and ovals represent synapses. Three parameters used in this study are shown. (B) Quantification of overlap between DA8 and DA9 synaptic domains in *unc-13* and axon guidance mutants. Error bars; standard error of mean. Triple asterisks; $p<0.001$ n.s.; not significant (ANOVA/Dunnett). (C-G) representative images of the synaptic patterns in DA8 and DA9 of wildtype (C); *unc-129* with DA8 misguided (D), DA9 misguided (E), or normal axon guidance (F); and *unc-13* mutants (G). Arrows denote the tiling border. Overlap between the DA8 and DA9 synaptic domains are indicated in yellow bars. Scale bar, 20μm. See also Figure S1.

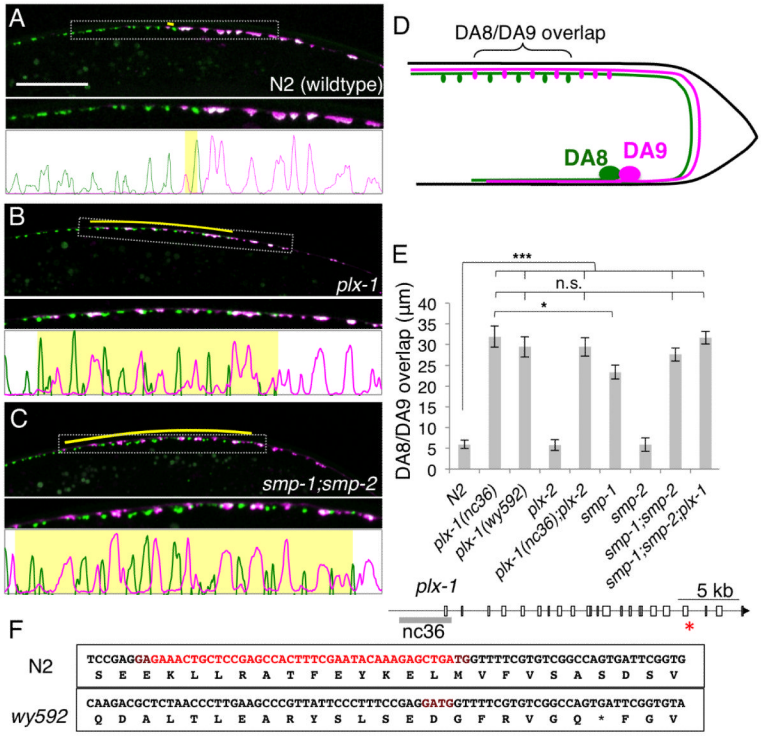

Figure 2. *plexin* and *semaphorin* mutants have synaptic tiling defects

(A-C) Synaptic tiling defect in L4 animals of wildtype (A) *plx-1(nc36)* (B) and *smp-1;smp-2* (C) mutants. Overlap between the DA8 and DA9 synaptic domains are indicated in yellow bars. Magnified images (represented by dotted boxes) and line-scan images within the magnified region were also shown. (D) Schematic representation of the tiling mutant phenotype. (E) Quantification of overlap between DA8/DA9 synaptic domains. Error bars; standard error of mean. Triple asterisks; $p<0.001$, Single asterisk; $p<0.05$ n.s.: not significant (ANOVA/Tukey-HSD). (F) Schematic representation of the genomic locus of the *plx-1* gene. White boxes represent exons. The grey bar represents the deletion in *nc36*. The res asterisk indicates the position of deletion found in wy592 allele. DNA and corresponding amino acid sequences around the deletion found in *wy592* of wildtype and *wy592* are shown in the boxes. Sequence deleted in *wy592* allele is shown in red. See also Figure S1 to S4.

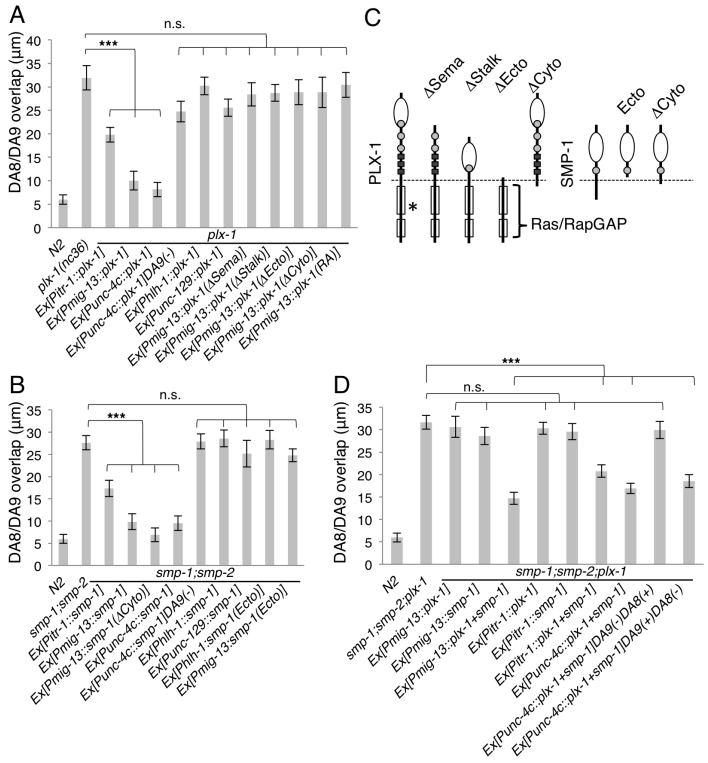

Figure 3. Both *plx-1* and *smp-1* function cell autonomously in DA9

(A) Cell specific rescue of *plx-1* with PLX-1 cDNA and its mutant variants expressed from cell-specific promoters. DA-specific (*Punc-4c*) and DA9-specific (*Pitr-1* and *Pmig-13*) PLX-1 expression rescued the tiling phenotype in the *plx-1* mutant. (B) Cell-specific rescue of *smp-1;smp-2* mutants by wild-type or mutant SMP-1 variants expressed from cell-specific promoters. DA-specific (*Punc-4c*) and DA9 specific (*Pitr-1* and *Pmig-13*) SMP-1 expression rescued DA8/9 synaptic overlap. (C) Schematics of PLX-1, SMP-1 and their deletion mutants used in this study. PLX-1 has one SEMA domain (white circle), three PSI domians (grey circles) and three glycine-proline rich repeats (black boxes) in the extracellular domain. There is a conserved RasGAP domain (white boxes) in the cytoplasmic domain. Asterisk indicates the position of deletion found in *wy592* allele. SMP-1 has one SEMA domain (white circle) and one PSI domain (grey circles). (D) Cell specific rescue of *smp-1;smp-2;plx-1* mutants with PLX-1 and/or SMP-1 cDNA. Expression of both PLX-1 and SMP-1 cDNA from DA9 specific promoters (*Pitr-1* and *Pmig-13*) rescued the triple mutants. Mosaic experiment using DA specific promoter (*Punc-4c*) was alsho shown. (−) indicates the loss of transgene in the cell. Triple asterisks: $p<0.001$, n.s.: not significant (ANOVA/Dunnett). Error bars; standard error of mean. See also Figure S5 to S7.

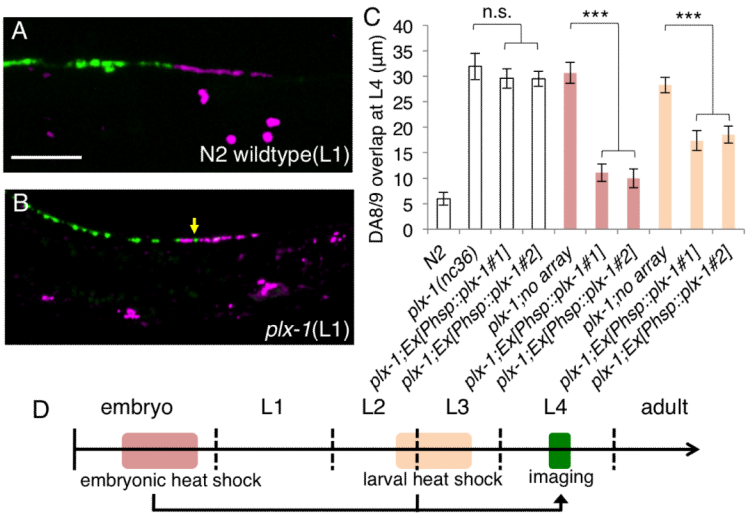

Figure 4. PLX-1 functions throughout development

(A and B) Synaptic tiling at early L1 stage of wild type (A) and *plx-1* mutants (B). A tiling defect was observed at this stage in the *plx-1* mutants (yellow arrow). Scale bar, 10μm. (C) Quantification of DA8/DA9 overlap at L4 stage. Two independent transgenic lines and their siblings without the transgenes were quantified. Heat shock induction of *plx-1* gene expression from the *hsp* promoter at the embryonic (red bars) and larval (orange bars) stages significantly rescued the *plx-1* mutant phenotype while there was no significant difference between transgenic animals and non-transgenic siblings without heat shock (white bars). Error bars; standard error of mean. Triple asterisks: $p<0.001$, n.s.: not significant (ANOVA/Tukey-HSD). (D) Schematic representation of worm developmental time course and the timing of heat shock and imaging.

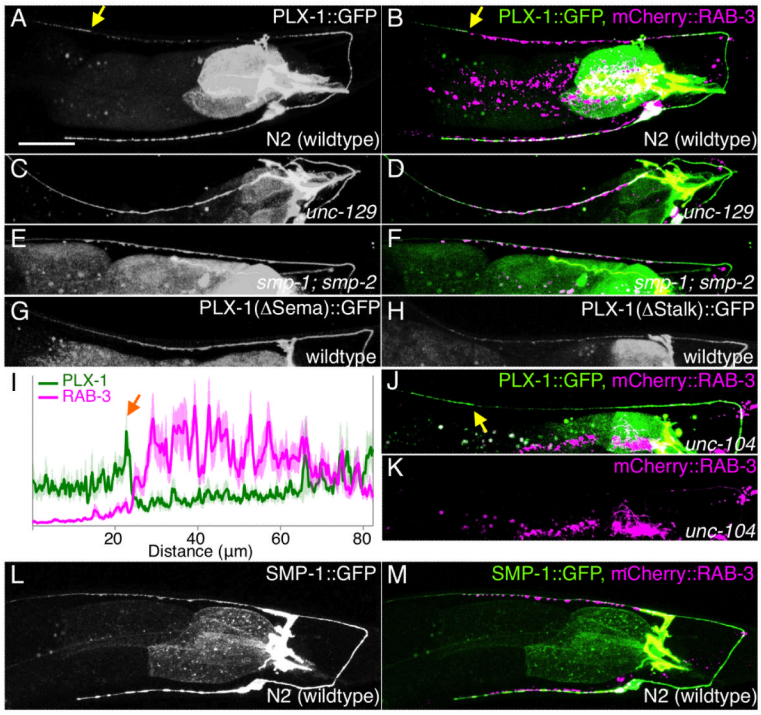

Figure 5. PLX-1::GFP is enriched at a synapse-free domain adjacent to the synaptic region

PLX-1::GFP localization in wildtype (A, B), in *unc-129* mutants with DA9 axon misguided (C, D) and in *smp-1;smp-2* mutants (E, F). Each strain has a synaptic marker (P*mig-13::mCherry::rab-3*) and merged images are shown in the right panel (B, D and F). (G) PLX-1(ΔSema)::GFP localization in wildtype. (H) PLX-1(ΔStalk)::GFP localization in wildtype. (I) Quantification of the normalized mCherry::RAB-3 signal (magenta) and PLX-1::GFP signal (green) in the dorsal axon of wildtype worms. 18 animals were aligned according to the PLX-1::GFP patch at the anterior edge of the DA9 synaptic domain (orange arrow). Light colors indicate standard error of mean. (J) PLX-1::GFP merged with mCherry::RAB-3 in *unc-104/kinesin* mutants. mCherry::RAB-3 signal is completely absent from the dorsal axon (K). PLX-1 at the putative tiling border is indicated by yellow arrows. (L) SMP-1::GFP localization in wildtype. (M) mCherry::RAB-3 co-labeled with SMP-1::GFP. Scale bar, 20μm.

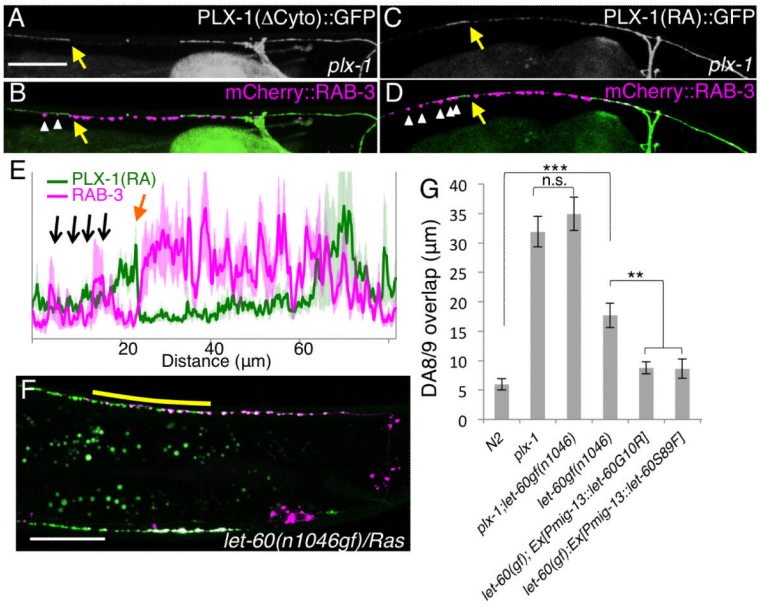

Figure 6. PLX-1 tiles synapses by inactivating Ras in DA9

(A-D) Subcellular localization of PLX-1 lacking its cytoplasmic domain (ΔCyto) (A and B) and RasGAP-deficient PLX-1 (PLX-1(RA)::GFP) in the *plx-1* mutants (C and D). PLX-1 signal at the putative tiling border is indicated by yellow arrows, and ectopic synapses (mCherry::RAB-3) in the anterior axon are indicated by white arrowheads in (Band D). (E) Quantification of the normalized mCherry::RAB-3signal (magenta) and PLX-1(RA)::GFP signal (green) in the dorsal axon of wildtype worms. 18 animals were aligned according to the PLX-1::GFP patch at the putative anterior edge of the DA9 synaptic domain (orange arrow). Black arrows indicate ectopic RAB-3 signal anterior to the PLX-1(RA) localization. The light-green and light-magenta traces indicate standard error of mean. Scale Bars, 20 μm. (F) Synaptic tiling defect in *let-60* (Ras) gain-of-function mutants. Yellow bar indicates DA8/DA9 synaptic overlap. (G) Genetic interaction between *plx*-1 and *let-60(gf)*, and cell-specific suppression of *let-60(gf)* by two dominant negative LET-60 mutants. Triple asterisks; $p<0.001$, Double asterisks; $p<0.01$, n.s.: not significant (ANOVA/Tukey-HSD). Scale bar, 20μm.

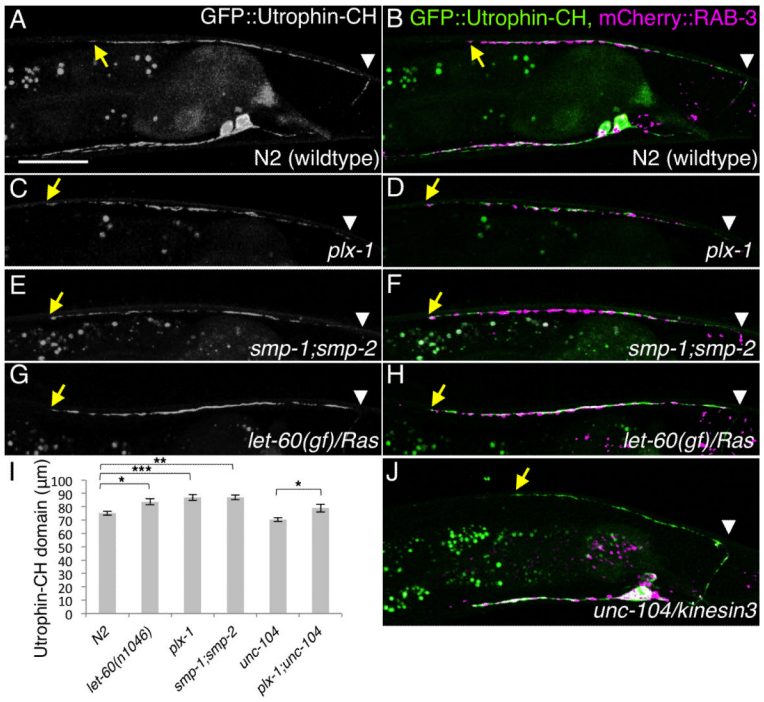

Figure 7. F-actin is enriched at the DA9 synaptic domain and is expanded in the synaptic tiling mutants

(A-H) GFP::Utrophin-CH pattern in DA9 of wildtype (A, B), *plx-1* mutants (C, D), *smp-1;smp-2* double mutants (E, F) and *let-60(n1046gf)* mutants (G, H), either GFP::Utrophin-CH signal alone (A, C, E and G), or overlaid with mCherry::RAB-3 (B, D, F and H). (I) Quantification of Utrophin-CH domains in the dorsal axon. The length of the Utrophin-CH domain from the most posterior-dorsal axon (indicated with white arrowheads) to the anterior edge (indicated with yellow arrows) was measured. Triple asterisks; $p<0.001$. Double asterisks; $p<0.01$, Single asterisk; $p<0.05$ (ANOVA/Tukey-HSD). Error bars; standard error of mean. (J) GFP::Utrophin-CH and mCherry::RAB-3 double labeling in *unc-104* mutants. Note that the mCherry::RAB-3 signal is completely absent in the dorsal axon. Scale bar, 20μm.

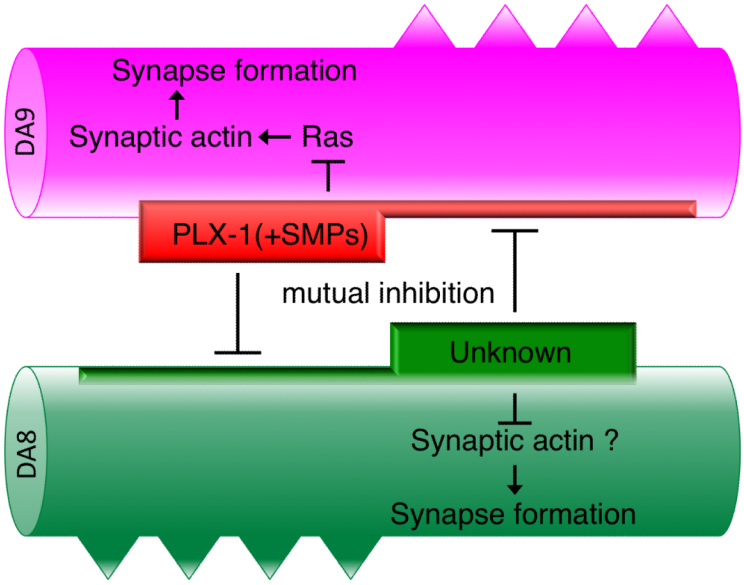

Figure 8. Model of the synaptic tiling in DA8/DA9

PLX-1 is localized at the synaptic tiling border dependent on both SMP-1 in DA9 and unknown molecule(s) in DA8. Localized and activated PLX-1 inhibits synapse formation in DA9 as well as restricts the activity or localization of unknown molecule(s) in DA8. See text for detail.